Alternative reinforcing details for precast concrete beams at cast-in-place beam-column connections

H.J. Lee & H.C. Chen

Department of Civil and Construction Engineering, National Yunlin University of Science and Technology, Yunlin, Taiwan.

J.H. Syu

Lee Ming Construction Co. Ltd, Taichung, Taiwan.

2017 NZSEE Conference

ABSTRACT: The paper presents an experimental investigation on alternative reinforcing details for bottom bars of precast concrete beams at cast-in-place beam-column joints to achieve behaviour as for monolithic reinforced concrete beam-column connections. To relief steel congestion and fabrication difficulty, it is proposed to use head bars for bottom bars protruded from precast beams and anchored in the middle of the beam-column joint. Six interior beam-column connection specimens were tested under reversed cyclic loading. The primary test variables were the anchorage of bottom beam bars in the joint and the presentence of transverse beams. Within the experimental programme, four connection specimens with bottom beam bars anchored in the middle of the joint performed as good as the other two benchmark specimens with continuous beam bars. Hysteretic behaviour, including strength degradation, stiffness degradation, and energy dissipation, were evaluated in accordance with acceptance criteria for special moment-resisting frames. On the basis of experimental results, design recommendations are drawn for such emulative precast beam-column connections.

1 INTRODUCTION

Many possible arrangements of precast concrete members and cast-in-place concrete forming ductile moment-resisting frames have been used in many countries (Park, 2002; Pampanin, 2005; Watanabe, 2007). Figure 1 shows the most commonly used arrangement of emulative precast beam-column connections in Taiwan. Precast beam elements are placed on the edges of bottom precast columns, and then the reinforcement is placed in the beam-column joint core, the top of the beams, and the slabs. Afterward, the cast-in-place concrete is placed to form an emulating monolithic reinforced concrete beam-column-slab connection.

This arrangement of precast elements leads to a large reduction on site formwork and labours, but also arise a difficulty of steel congestion within the cast-in-place joint, where the bottom beam bars, protruding from the precast beam elements, need to be extended to the far face of joint core and bent up for anchorage. Hence the bottom beam bars framing from two opposite faces of a joint have to be well staggered in order not to overlap each other. Even so, the bent-up hook extensions of bottom beam bars may conflict with the inner ties within the joint core. Due to steel congestion, the quality of cast-in-place concrete in the joint core may be questioned.

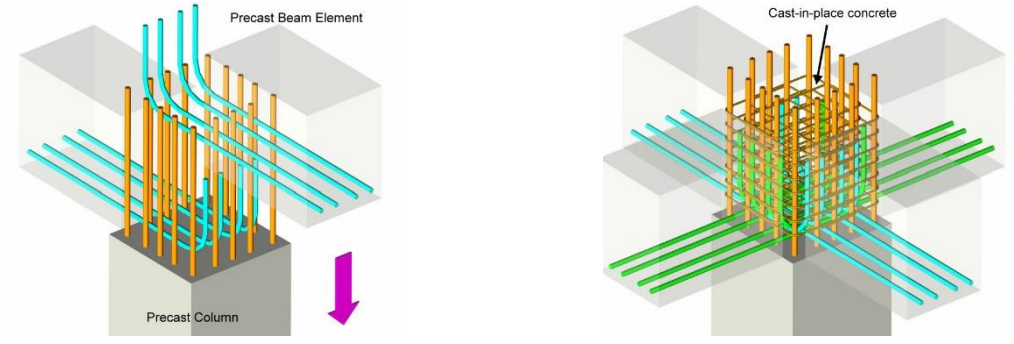

Figure 1. Conventional arrangement for connecting precast beams at a cast-in-place joint.

The use of headed reinforcement provides a promising way to ease the steel congestion in a beam-column joint (Wallace et al., 1998; Kang et al., 2009). This paper proposes alternative reinforcing details to terminate bottom beam bars at the joint middle with anchored plates or heads, provided that the headed bars have adequate anchorage length and confined with closely-spaced joint hoops and ties. The proposed alternative reinforcing details of bottom beam bars could liberate the difficulties in the design, erection, and fabrication of the precast beam elements at cast-in-place beam-column joints, as shown in Figure 2. To verify this idea, an experimental programme was conducted to investigate the use of headed bottom beam bars terminated in the joint middle in comparison with the conventional design.

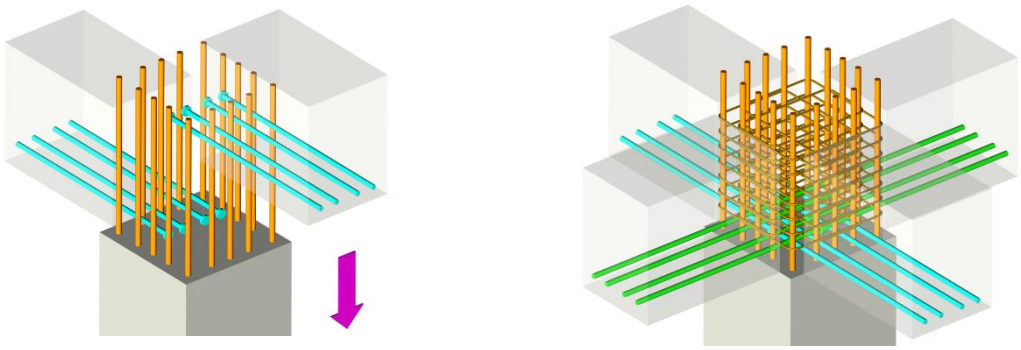

Figure 2. Proposed alternative reinforcing details for connecting precast beams at a cast-in-place joint.

2 TEST PROGRAMME

2.1 Connection design

Six emulative precast beam-column connections were tested under reversed cyclic loading. Figure 3 shows the matrix of test specimens. Three joint specimens, designated as Group A, used eight and four D25 reinforcing bars for the longitudinal reinforcement in the beam top and bottom, respectively, resulting in an unequal reinforcement ratio in the beam section. The other three specimens, designated as Group B, used six D25 reinforcing bars symmetrically for the top or bottom beam reinforcement. The total amount of beam longitudinal reinforcement are 12 D25 reinforcing bars, and thus the design shear force of the joint (V_u), which is estimated by the method recommended by ACI 352R-02 (ACI-ASCE Committee 352, 2002), is approximately equal to 2720 kN for each test connection.

$$V_u = 1.25f_y\left(A_{s,top} + A_{s,bot}\right) - V_{col} \quad (1)$$

$$V_{col} = \frac{\left(M_{pr}^{+} + M_{pr}^{-}\right)}{\left(L_b - h_c\right)}\frac{L_b}{L_c} \quad (2)$$

where $A_{s,bot}$ is the area of bottom beam bars; $A_{s,top}$ is the area of top beam bars; f_y is the specified yield strength of reinforcement; V_{col} is the column shear force in equilibrium with the probable beam moments M_{pr} at the joint faces, which were determined using a bar stress of $1.25f_y$, for positive and negative bending moments, respectively; L_b is the unit beam length (4.5 m for tested specimens); L_c is the unit column length (3 m for tested specimens) or the equivalent story height; h_c is the column depth of 500 mm.

All test specimens had a square column section of 500x500 mm detailed with 12 D25 Grade 420 longitudinal reinforcing bars and D13 Grade 490 transverse hoops and ties at a spacing of 100 mm. The Grade 490 reinforcement was used to reduce the amount of transverse reinforcement for confinement of 55-MPa concrete column.

Table 1 shows the material properties and connection design parameters calculating using ACI 352R-02 method for each test specimen. The measured yield and ultimate strengths of flexural reinforcement are 470 MPa and 670 MPa, respectively. All specimens were designed to meet the requirements for special moment frames per ACI 318, except the alternative details of bottom beam bars, which are examined in this program. The design shear stress acting on the joint is controlled to be $1.67\sqrt{f_c'}$ MPa, which is specified value for interior joints confined on all four faces. In other words, the design joint shear for Specimen A3 or B3 was aimed to at the limiting shear strength specified in ACI 318, while the

design joint shear in other four cruciform specimens were designed to exceed the limiting value of $1.25\sqrt{f_c'}$ MPa for interior joints without transverse beams.

Joint transverse hoops and ties are proportioned according to ACI 318 code, which requires special transverse reinforcement to be extended throughout the joint and adjacent column ends, unless a joint is considered to be effectively confined by beams on all four sides, such as Specimens A3 and B3.

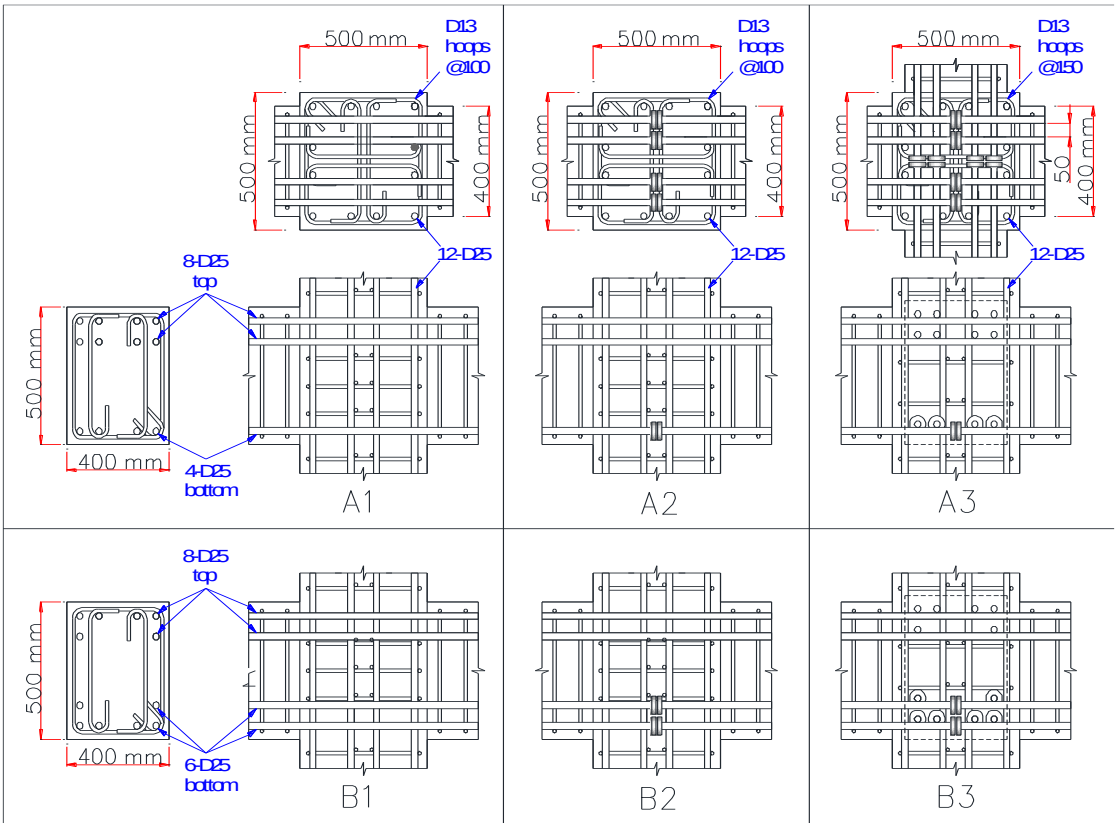

Figure 3. Test matrix of beam-column joint specimens.

Table 1. Material properties and connection design parameters.

Parameter \ Specimen	A1	A2	A3	B1	B2	B3
Concrete strength f_c' (MPa)	56.8	61.9	49.2	55.6	51.2	53.2
Flexural strength ratio M_r*	1.27	1.28	1.26	1.27	1.27	1.27
Target joint shear V_u (kN)	2717	2717	2717	2721	2721	2721
Confinement ratio $\frac{A_{sh}}{sb_c}$**	0.0112	0.0112	0.0075	0.0112	0.0112	0.0075
Trans. beam confinement	NA	NA	Yes	NA	NA	Yes

*Column-to-beam flexural strength ratio=$\Sigma M_{nc}/\Sigma M_{nb}$, where ΣM_{nc} and ΣM_{nb} are the sum of the nominal moment strengths of the columns and beams, respectively, calculated at the joint faces.

**Where A_{sh} is the total cross-sectional area of the transverse reinforcement, including crossties, within spacing s and perpendicular to dimension b_c, which is the cross-sectional dimension of the column core without concrete cover.

For Grade 420 straight beam bars passing through the joint, ACI 318 and ACI 352R-02 require a minimum column depth of 20 bar diameters ($20d_b$) for joints of special moment frames. All test connections shown in Figure 3 used Grade 420 25-mm-diameter longitudinal reinforcing bars and a

column depth of 500 mm, which is approximate to $20d_b$. For headed deformed bars anchored in the joints of special moment frames, ACI 318 gives a minimum development length, measured from the beam-column interface to the bearing face of the head, as follows.

$$\ell_{dt} = 0.19 f_y d_b / \sqrt{f_c'} \quad (3)$$

with limitations of (a) specified f_y not exceeding 420 MPa; (b) bar size not exceeding 36 mm; (c) normal-weight concrete; (d) Each head has a net bearing area exceeding 4 times the nominal cross-sectional area of the bar; (e) minimum clear cover of $2d_b$ for each bar; and (f) minimum clear spacing of $3d_b$ between parallel bars.

Substituting bar f_y of 420 MPa and design concrete strength f_c' of 55 MPa into Eq. (3) resulting in a minimum development length of $10.8d_b$. The provided development length of the headed bars is only $9d_b$, measured from the bearing face of the head to the column face. Furthermore, all test specimens were detailed with longitudinal beam bars at a clear spacing of $2d_b$ between bars. Obviously, the anchorage conditions of the bottom beam bars used in this test program are relatively severe.

Kang et al. (2009) extensively reviewed previous research on the use of headed bars in reinforced concrete beam-column joints and concluded that the minimum clear spacing between headed bars can be reduced to $2d_b$. Also, the ℓ_{dt} of Eq. (3) is relatively much more conservative for headed bars in beam-column joints. Four exterior beam-column joint specimens with staggering headed bars at a clear spacing of $1.2d_b$ tested by Lee and Yu (2007) did demonstrate adequate anchorage capacities. Based on prior experimental evidence, this study used $2d_b$ for headed bar spacing.

2.2 **Test setup and procedure**

Figure 4 shows the setup for the reversed cyclic loading test of an isolated cruciform beam-column assemblage. The column base was pin-connected on strong floors. At the beginning of test, a column axial load of $0.05A_g f_c'$ was applied via four pretension rods aside the column. During testing, the column axial load was manually held around the target value of $0.05A_g f_c'$. The free ends of the beams were tied down to the strong floor to simulate the inflection points of the beam. The test setup was arranged to eliminate the P-delta effect and to simulate a 3/4-scale beam-column joint specimen with a column height (story height) of 3 m and a beam span of 4.5 m (the distance between the roller-supported inflection points).

Figure 4. Test set-up photo.

A typical displacement-controlled loading protocol consisting of three reversed cycles at gradually increased drift ratios (0.50%, 0.75%, 1.0%, 1.5%, 2%, 3%, 4%, 6%, and 8%) was used in this study. The target displacement at the loading point of the upper column was computed by multiplying the target drift ratio to the simulated story height of 3000 mm. The axial load and lateral force at the upper column were monitored by load cells. Several displacement transducers were attached to the test specimen to measure the global lateral drifts and local deformations. Numerous strain gauges were pre-attached to reinforcements at key locations to record the strain histories. In general, the loading protocol and test

procedure in this experimental program are consistent with respect to ACI 374.1-05(ACI Committee 374, 2005). The presented test results herein continued up to 6% or 8% drift ratio for the observation of failure modes. However, the performance of test specimens should be evaluated prior to the limiting drift ratio of 4%, because the 6% or 8% drift may be too large for a well-designed special moment frame.

3 TEST RESULTS AND DISCUSSION

3.1 Cyclic loading response

Figure 5 shows the hysteretic, skeleton, and backbone curves for all test specimens. Specimens A1 and B1 are benchmark specimens with continuous bottom beam bars. The yielding of beam bars occurred in the cycle of 1.5% drift, followed by the maximum loads measured at the drift ratio of 3% and the significant joint distortion. The applied lateral load (Q) was normalized to the theoretical lateral resistance (Q_n) obtained from measured material properties and a strain compatibility analysis for flexural strengths of the beams at critical section. As shown in Figure 5, the maximum lateral resistances recorded in Specimens A1 and B1 were greater than Q_n, but fall below Q_n at the 6% drift cycles due to the joint shear failure. The failure mode of Specimens A1 and B1 was joint shear failure after beam yielding.

Specimen A2 and B2 exhibited similar behavior and failure modes with respect to Specimen A1 and B1. As compared in Figures 6 and 7, the cyclic response of Specimen A2 was almost identical to that of Specimen A1. On the other hand, the performance of Specimen B2 was somewhat inferior to that of Specimen B1. Based on testing observation and comparison, it is concluded that the proposed alternative details for bottom beam bars can be used if following conditions were satisfied. Firstly, the ratio of bottom-to-top flexural reinforcement is about 0.5. Secondly, the joint is well confined with joint transverse reinforcement. Finally, the anchorage length of the headed bars should be sufficient to preclude the breakout failure.

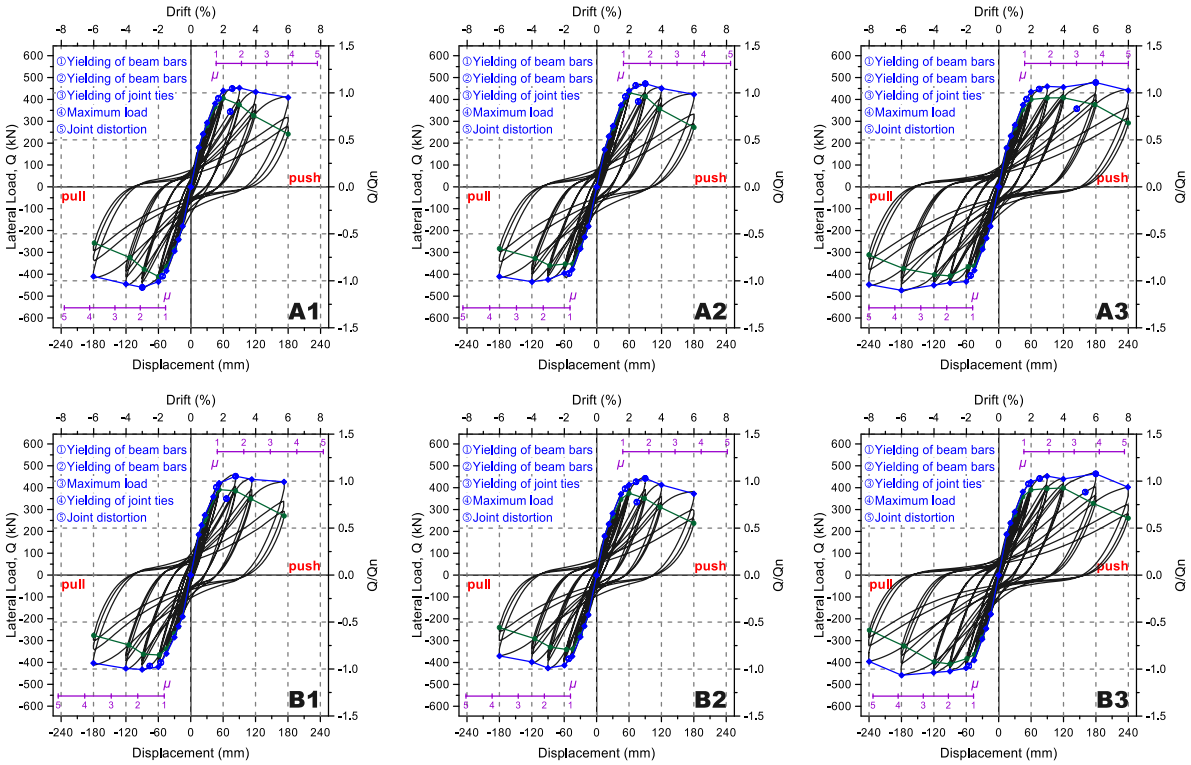

Figure 5. Hysteretic, skeleton, and backbone curves of tested units.

As shown in Figures 5, the performance of Specimens A3 and B3, which were confined on all four faces, were obviously better than those of other four cruciform specimens. Due to the enhancement of transverse beams to the joint, Specimens A3 and B3 attained the maximum lateral resistances at the drift ratio of 6%, which is more than enough for a well-designed moment resisting frame. The cyclic loading

tests of Specimens A3 and B3 were therefore continued to finish the 8% drift ratio to observe failure modes. Figure 6 shows the final damage stage of Specimen B2 at the end of 6% drift cycles and that of Specimen B3 at the end of 8% drift cycles. Due to the confinement of the transverse beams, the joint damage in Specimen B3 is less than that in Specimen B2. On the other hand, Specimen B3 had well-developed beam plastic hinges adjacent to the joint.

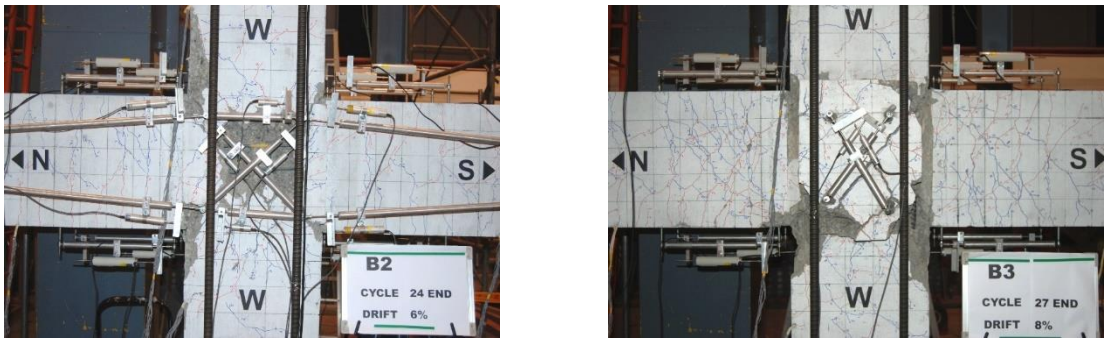

Figure 6. Final damage patterns of Specimen B2 and B3.

3.2 **Anchorage performance of bottom beam bars**

Figure 7 shows the strain profiles along the bottom beam bars at peak drift ratios for the four cruciform specimens. All beam bar strains measured at the beam-column faces (location at ± 250 mm) went above the ideal yield strain of 2155 με (measured from bar tensile test) at the 2% drift ratio indicating the development of beam yielding. For Specimen A1 and B1, a clear strain gradient per distance along the straight beam bar passing through the joint can be observed in Figure 7. This indicated that the bond resistance in the joint had not been completely destroyed till the 3% drift ratio. It is concluded that the development length of $20d_b$ is adequate for the straight beam bars used in the test specimens.

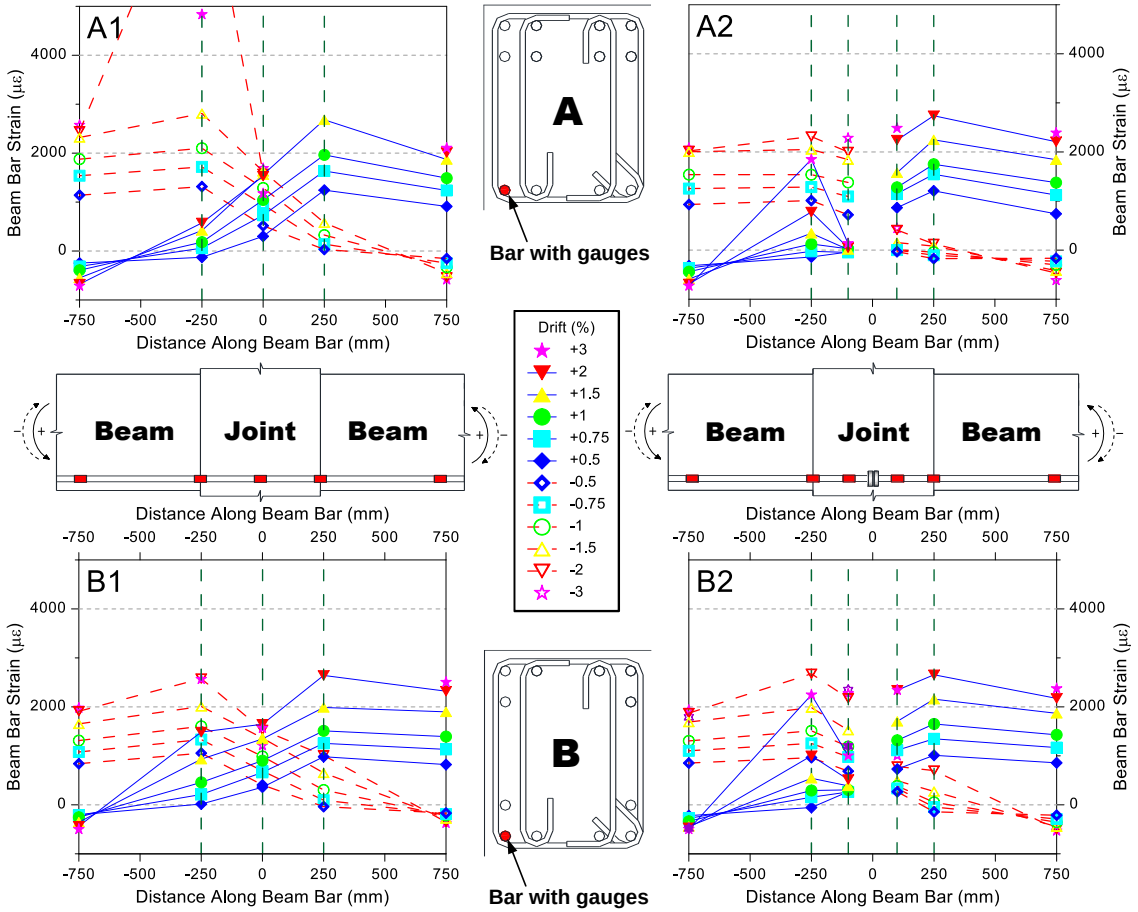

Figure 7. Profiles of strain developed along bottom beam bars for test specimens.

For Specimens A2 and B2 with alternative reinforcing details, the beam bar strains measured at the beam-column faces (location at ± 250 mm) and in the joint core (location at ± 100 mm) exceeded the bar yield strain at the 2% drift ratios indicating almost the entire bar tensile force was transferred to the end anchorage. It is evident that the bottom beam bars in Specimen A2 and B2 were effectively anchored by heads with a short anchorage length and a clear spacing of $2d_b$ in the beam-column joints. Notably, the joints were well detailed with transverse reinforcement.

3.3 **Profiles of tie bar stress**

Figure 8 compares the profiles of tie bar strains measured at one top column crosstie (Gauge 11) above the top beam bars, three inner joint crossties (Gauges 12-14) between the top and bottom beam bars, and another bottom column crosstie (Gauge 15) below the bottom beam bars for the cruciform test specimens. Each gauge was attached to the centre of the crosstie parallel to the beam bars. Figure 8 shows that the tie bar strains measured in the joint (Gauges 12-14) remained elastic in the 1.5% drift cycles but went beyond the yield strain of 2500 με at the 2% drift ratios for all test specimens. Notably, the tie bar strains measured in the top and bottom column (Gauges 11 and 15) remained elastic over the entire loading history in Specimens A1 and B1 with continuous bottom beam bars.

In contrast, the tie bar strains measured below the discontinuous bottom beam bars in Specimens A2 and B2 (Gauge 15) went beyond the yield strain of 2500 με after the 2% drift cycles. Besides, the tie bar strain of Gauge 14 in Specimen B2 was relatively larger than that of Gauge 14 in Specimen B1 for each drift level. These phenomena can be explained using Figure 9, where the tensile force of the bottom beam bars was transferred to the transverse reinforcement in the joint and the bottom column.

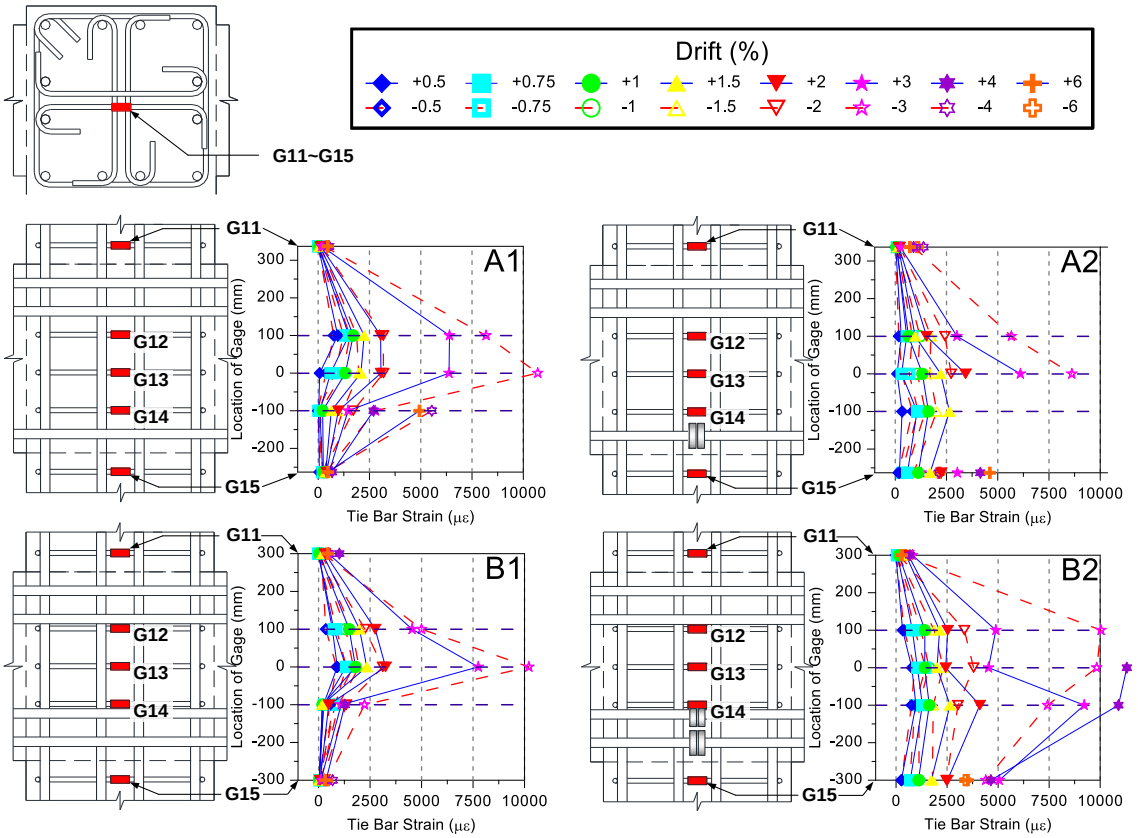

Figure 8. Profiles of tie bar strain along column height.

4 **DESIGN RECOMMENDATIONS**

For the anchorage of the bottom beam bars by heads in the middle of the joint, yielding of the column transverse reinforcement is not preferred because it may affect the column confinement. Therefore, it is recommended to provide one more set of joint transverse reinforcements below the bottom beam bars anchored in the joint, as shown in Figure 9. To preclude breakout failure, this paper recommends that

the total amount of joint and column transverse reinforcement covered by the fan-shaped struts should be capable of resisting the total tensile force to be developed in the bottom beam bars.

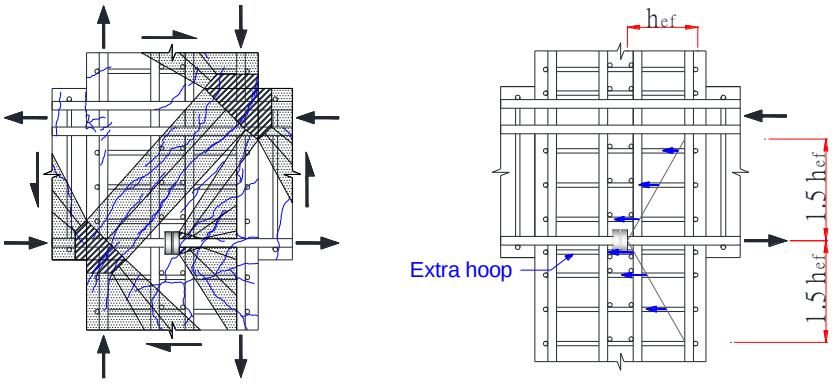

Figure 9. Strut-and-tie modelling for precluding the concrete breakout failure.

5 CONCLUSIONS

The experimental results presented in this work demonstrated that emulative precast beam-column connections with bottom beam bars anchored in the joint middle can perform as well as monolithic beam-column connections with straight beam bars passing through the joint. Based on standard testing protocol and performance evaluation, it is concluded that it is a viable option to terminate bottom beam bars at the middle of a well-confined joint with adequate heads, practical clear spacing of $2d_b$, and sufficient anchorage length. From the experimental observations, the potential for concrete breakout failure increased for the closely spaced headed bars that were used in the test specimens. To preclude breakout failure, adequate transverse reinforcement should be provided and distributed uniformly within the critical edge distance of 1.5 times the effective embedded depth of the headed bars in the confined core. The amount of transverse reinforcement could be proportioned by establishing load paths in accordance with strut-and-tie modelling principles.

6 REFERENCES

ACI-ASCE Committee 352. 2002. *Recommendations for Design of Beam-Column Connections in Monolithic Reinforced Concrete Structures (ACI 352R-02)*. Retrieved from Farmington Hills, MI:

ACI Committee 318. 2014. *Building Code Requirements for Structural Concrete (ACI 318-14) and Commentary*. Farmington Hills, MI: American Concrete Institute.

ACI Committee 374. 2005. *Acceptance Criteria for Moment Frames Based on Structural Testing and Commentary (ACI 374.1-05)*. Retrieved from Farmington Hills, MI:

Kang, T.H.K., Shin, M., Mitra, N., & Bonacci, J.F. 2009. Seismic Design of Reinforced Concrete Beam-Column Joints with Headed Bars. *ACI Structural Journal*, 106(6), 868-877.

Lee, H.J., & Yu, S.Y. 2009. Cyclic Response of Exterior Beam-Column Joints with Different Anchorage Methods. ACI Structural Journal, 106(3), 329-339.

Pampanin, S. 2005. Emerging solutions for high seismic performance of precast/prestressed concrete buildings. *Journal of Advanced Concrete Technology*, 3(2), 207-223.

Park, R. 2002. Seismic Design and Construction of Precast Concrete Buildings in New Zealand. *PCI Journal*, 47(5), 60-75.

Wallace, J.W., McConnell, S.W., Gupta, P., & Cote, P.A. 1998. Use of headed reinforcement in beam-column joints subjected to earthquake loads. *ACI Structural Journal*, 95(5), 590-606.

Watanabe, F. 2007. Design of Precast Concrete Buildings Emulating Monolithic Construction. *Proceeding of The Ninth Japan-Korea-Taiwan Joint Seminar on Earthquake Engineering for Building Structures (SEEBUS 2007)*, Hsinchu, Taiwan.